

Vortex quantum creation and winding number scaling in a quenched spinor Bose gas

Michael Uhlmann¹, Ralf Schützhold^{1,†} and Uwe R. Fischer^{2,✉}

¹*Institut für Theoretische Physik, Technische Universität Dresden, D-01062 Dresden, Germany*

²*Eberhard-Karls-Universität Tübingen, Institut für Theoretische Physik
Auf der Morgenstelle 14, D-72076 Tübingen, Germany*

Motivated by a recent experiment, we study non-equilibrium quantum phenomena taking place in the quench of a spinor Bose-Einstein condensate through the zero-temperature phase transition separating the polar paramagnetic and planar ferromagnetic phases. We derive the typical spin domain structure (correlations of the effective magnetization) created by the quench arising due to spin-mode quantum fluctuations, and establish a sample-size scaling law for the creation of spin vortices, which are topological defects in the transverse magnetization.

PACS numbers: 03.75.Mn, 73.43.Nq, 03.75.Lm, 05.70.Fh.

A rapid sweep through a symmetry-breaking zero-temperature phase transition entails fascinating non-equilibrium quantum phenomena. The quench generates causally disconnected spatial domains of different order parameter values (corresponding to positions in the new ground-state manifold), which may ultimately form topological defects in a quantum version of the Kibble-Zurek mechanism [1, 2, 3]. Apart from its relevance in condensed-matter theory (e.g., in superconductors, these defects affect measurable transport properties like conductivity and susceptibility) and potentially cosmology [2], this phenomenon is very interesting from a fundamental point of view, since the defect distribution directly originates from the initial quantum fluctuations and thus maps out their properties (such as the ground-state entanglement).

Because of their comparably long response times, dilute atomic gases provide a unique opportunity for exploring these fundamental quantum many-body phenomena far from equilibrium in the laboratory. In the following, we derive the spectrum of fluctuations induced by a rapid quench to the (planar) ferromagnetic state of a spinor Bose gas, and establish a general sample-size dependent scaling law for the resulting variance of the net number of spin vortices (i.e., of the winding number). Besides the total defect density, the winding number within a given area determines the spectrum of the created magnetization fluctuations. Thus dilute Bose gases serve as a useful and experimentally accessible toy model for the general case and may allow us to extract universal properties of such dynamical phase transitions.

Spinor Bose-Einstein condensates are created by trapping different hyperfine states of a particular atomic species by optical means [4], which enables, *inter alia*, the investigation of coherent spin-exchange dynamics [5], and the formation of spin domains by a dynamical instability [6]. Non-equilibrium phenomena in a spinor Bose gas were realized in a recent experiment [7], where an initially paramagnetic state was rapidly quenched through a quantum phase transition to a final ferromagnetic state [8]. Such a quench results in spin vortices, (imaged *in situ*

by phase contrast techniques [9]), which are topological defects in the magnetization with a paramagnetic core [10, 11]. The dilute spinor Bose gas can be described in terms of multi-component field operators $\hat{\psi}_a$, whose dynamics is governed by the Hamiltonian density ($\hbar = 1$)

$$\hat{H} = \frac{1}{2m} (\nabla \hat{\psi}_a^\dagger)^2 + \hat{\psi}_a^\dagger V_{\text{trap}} \hat{\psi}_a + \frac{c_0}{2} \hat{\psi}_a^\dagger \hat{\psi}_b^\dagger \hat{\psi}_b \hat{\psi}_a + \frac{c_2}{2} \hat{\psi}_a^\dagger \hat{\psi}_b^\dagger \hat{\psi}_c \hat{\psi}_d + \frac{q}{2} \hat{\psi}_z^\dagger \hat{\psi}_z; \quad (1)$$

where m denotes the mass of the atoms. The vector \mathbf{F}_{ab} contains the spin matrices [12] and determines the effective magnetization $\hat{\mathbf{F}} = \mathbf{F}_{ab} \hat{\psi}_a^\dagger \hat{\psi}_b = \frac{\hbar}{2} \hat{\rho}$, where a summation over component indices a, b, c, d is implied and $\hat{\rho} = \hat{\psi}_a^\dagger \hat{\psi}_a$ is the total (conserved) density. For spin-one systems, the sum runs over $a = 0, \pm 1$ or, alternatively, over $a = x, y, z$ with $\hat{\rho} = \hat{\psi}_0^\dagger \hat{\psi}_0 + \hat{\psi}_x^\dagger \hat{\psi}_x + \hat{\psi}_y^\dagger \hat{\psi}_y + \hat{\psi}_z^\dagger \hat{\psi}_z = 2$. The coupling constants $c_0 = 4(a_0 + 2a_2)/(3m)$ and $c_2 = 4(a_2 - a_0)/(3m)$ are determined by scattering lengths a_S for the scattering channel with total spin S . For $c_0 \ll \bar{\rho}$ density fluctuations are energetically suppressed in comparison with the spin modes. Since we are interested in the effects of the phase transition (which is, strictly speaking, only well-defined for infinite systems) and not in the impact of inhomogeneities, we assume $\bar{\rho} = \text{const.}$ and hence omit the scalar trapping potential V_{trap} . Finally, q denotes the strength of the quadratic (one-particle) Zeeman shift $q \hat{\psi}_z^\dagger \hat{\psi}_z$ [7], where an external magnetic field is oriented along the z direction. (The linear Zeeman shift can be eliminated by transforming to the co-rotating frame, because the Larmor precession is much faster than all other frequency scales [10].)

Assuming $c_2 < 0$, the system is ferromagnetic for vanishing Zeeman shift $q = 0$, i.e., the magnetization $\hat{\mathbf{F}}$ assumes a maximum value $|\hat{\mathbf{F}}|^2 = 1$ in some given but arbitrary direction (broken-symmetry phase). For small but non-zero q the magnetization $\hat{\mathbf{F}}$ lies in the x, y -plane due to the term $q \hat{\psi}_z^\dagger \hat{\psi}_z$ but is still maximal, $|\hat{\mathbf{F}}|^2 = 1$. For large q however, the ground state corresponds to a condensate in the $\hat{\psi}_0 = \hat{\psi}_z$ component only and symmetry is restored, i.e., the magnetization $\hat{\mathbf{F}}$ vanishes (“para-

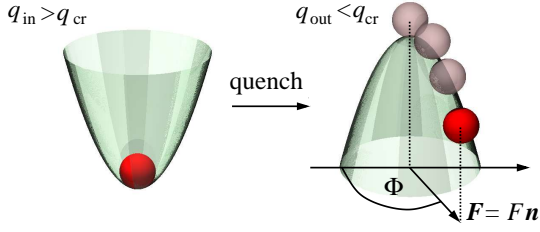


FIG. 1: Inversion behavior of the effective potential from (2). After crossing the critical point, the direction \mathbf{n} of the effective magnetization \mathbf{F} in the plane, at any given point in space, gets frozen at a particular angle Φ , while its modulus F continues to grow exponentially in time (“rolls down” the potential hill).

magnetic” phase). Hence, by rapidly lowering q , we may quench the system from an initially paramagnetic to an (effectively two-dimensional) ferromagnetic phase.

In order to study the evolution of the quantum field during the quench, we employ a number-conserving mean-field ansatz [13] $\hat{\mathbf{z}} = (\hat{c}_0 + \hat{\mathbf{z}})\hat{\mathbf{A}} = \hat{\mathbf{N}}$, which is adapted to the initial paramagnetic phase but can be extrapolated for some finite time after the quench [14], as long as the quantum fluctuations are small enough $\hat{\mathbf{x}}; \hat{\mathbf{y}}; \hat{\mathbf{z}} \ll \hat{c}_0$. This ansatz allows for a linearized expression for the magnetization (which assumes in Cartesian coordinates the simple form $\hat{\mathbf{F}}_a = i\hat{a}_{bc} \hat{c}_b \hat{c}_c$) and to derive an effective mean-field Hamiltonian for transverse magnetization $\hat{\mathbf{F}}$ from the full Hamiltonian Eq. (1),

$$\frac{\hat{H}_e}{\hbar} = \frac{\hbar}{2m} \nabla^2 + \frac{\hbar}{4} \nabla^2 + \hat{\mathbf{F}} \cdot \frac{q + 2c_2}{4} \nabla^2 + \hat{\mathbf{F}}; \quad (2)$$

with $\hat{\mathbf{z}} = (\hat{c}_0 \hat{y} + \hat{c}_0 \hat{y}; \hat{c}_0 \hat{x} - \hat{c}_0 \hat{x}) = 2$ being the canonical momentum operator for spin-one bosons. The experiment [7] is described by a two-dimensional transverse magnetization $\hat{\mathbf{F}} = (\hat{F}_x; \hat{F}_y)$ obeying the $SO(2)$ -symmetry of rotations around the z -axis in effectively two spatial dimensions $[\mathbf{r} = (x; y)]$, permitting topological defects in the form of spin vortices. However, the above expressions for the Hamiltonian are completely analogous for a $SO(N)$ -symmetry of the order parameter $\hat{\mathbf{F}}$ in $N > 2$ spatial dimensions, where the analogous topological defects are generically called “hedgehogs”, see, e.g., [15, 16, 17, 18]. Therefore, we shall discuss the general $SO(N)$ situation in the following and return to the experimentally realized example $N = 2$ of [7] at the end.

The simple expression (2) allows us to directly read off the critical value $q_{cr} = 2j_2^2/8m$ of the phase transition. After a quench from $q_{in} > q_{cr}$ to $q_{out} < q_{cr}$, and using a normal-mode expansion, we obtain exponentially growing modes corresponding to imaginary frequencies $\omega_k^q = (k + q)(k + q + 2c_2/8m)$, where $k = k^2/(2m)$, cf. Fig. 1. There are two regimes: For $q_{cr} > q_{out} > q_{cr}=2$, the exponential growth rate ω_k^q of the normal modes increases with their wavelength, but for $q_{out} < q_{cr}=2$, the

growth rate assumes its maximum at a given wavenumber $k_{max} = \frac{q}{2m(q_{cr} - 2q_{out})}$. In view of the experimental parameters [7], we shall focus on the second case. Note that due to the emergence of this preferred length scale, which is independent of the quench time, the present situation is somewhat different from the “standard” Kibble-Zurek scenario [1, 2], which is based on the interplay between quench time, relaxation rate, and correlation length.

Assuming the Bose gas to be sufficiently dilute, we may extrapolate our linearized (mean-field) description (2) to intermediate times t which contain many e -foldings $\omega_k^q \gg 1$ of the exponentially growing modes [14], whereas the magnetization is still small enough, $F^2 \ll 1$, to stay in the linear regime. After a normal-mode expansion, the expectation value $\langle \hat{\mathbf{F}}_a(\mathbf{r}) \hat{\mathbf{F}}_b(\mathbf{r}^0) \rangle$ contains exponentially growing contributions $\exp(i\omega_k^q t)$. In the limit $\omega_k^q \gg 1$, the $d^N k$ -integrals are dominated by the fastest-growing modes and can thus be approximated via the saddle-point method. Since the initial state (paramagnetic phase) is supposed to be globally isotropic such as the thermal ensemble or the ground state of (2), the dominant contribution to the two-point magnetization correlation function is calculated to be

$$\langle \hat{\mathbf{F}}_a(\mathbf{r}) \hat{\mathbf{F}}_b(\mathbf{r}^0) \rangle = C_{max} \frac{\exp(i\omega_{k_{max}} t) J_1(k_{max} |\mathbf{r} - \mathbf{r}^0|)}{k_{max} |\mathbf{r} - \mathbf{r}^0|}; \quad (3)$$

where J_1 is the Bessel function of the first kind with the index $\nu = N/2 - 1$. (The two-dimensional case was also considered in [7, 19].) Note that the above result is universal: Apart from C_{max} and k_{max} , all information enters the pre-factor C_{max} only, which depends on q_{out} , sweep rate, and temperature etc.

Now let us study the creation of topological defects, i.e., $SO(N)$ -hedgehogs, by the symmetry-breaking quench. Their characteristic size, i.e., the extent of the paramagnetic core, can be determined by comparing the kinetic term $\frac{\hbar}{2m} \nabla^2$ with the c_2 -contribution in (1) which yields $\xi_s = 1/\sqrt{2j_2^2/8m} = 1/\sqrt{m(q_{cr} - 2)}$, i.e., the spin healing length. In order to deal with well-separated and therefore well-defined topological defects, we assume that the dominant wave-length $\lambda_{max} = 2\pi/k_{max}$ (determining their typical distance, see below) is much larger than the spin healing length ξ_s , which amounts to requiring $0 < q_{cr} - 2q_{out} < q_{cr}$. This condition is reasonably well satisfied in the experiment [7] where $\xi_s \approx 2.4 \mu m$ and $\lambda_{max} \approx 16 \mu m$. Within the saddle-point approximation (i.e., focusing on the dominant modes), the term $\frac{\hbar}{2m} \nabla^2$ in the equations of motion resulting from (2) can be neglected compared to $q_{cr} - k_{max}^2/8m$, and we may approximate $F = \sqrt{q_{cr} - k_{max}^2/8m}$, and we may approximate $F = \sqrt{q_{cr} - k_{max}^2/8m}$. Consequently, at each spatial position, the magnetization \mathbf{F} behaves as the coordinate of a harmonic oscillator (in N dimensions), becoming inverted upon crossing the transition, cf. Fig. 1. Splitting \mathbf{F} up into its modulus F and unit vector of direction \mathbf{n} via $\mathbf{F} = F \mathbf{n}$, we find that F grows exponentially whereas the dynamics of \mathbf{n} freezes: In view of the

conserved “angular momentum” $L = \mathbf{F} \times \mathbf{E}$, we find that $\dot{\mathbf{j}} = \dot{\mathbf{L}} \times \mathbf{F}^2 / F_0^2 = \dot{\mathbf{F}} \times \mathbf{F}^2(t)$ decreases rapidly. Ergo, after a short time (of order $1/\omega_r$), the magnetization \mathbf{F} at each spatial position \mathbf{r} grows exponentially in some given direction $\mathbf{n}(\mathbf{r})$, i.e., the system rolls down the parabolic potential hill whereby the direction of descent does not change anymore, cf. Fig. 1. The correlations between the frozen directions \mathbf{n} at different spatial positions are governed by the initial state and determine the seeds for the creation of topological defects – i.e., objects which cannot be deformed to a constant \mathbf{n} in a smooth way [16].

The topological defects we are considering are $SO(N)$ (anti-)hedgehogs in N spatial dimensions with the typical order parameter distribution $\mathbf{n} = \mathbf{r}/r$ and can be characterized by a non-vanishing winding number, i.e., a topological invariant or “charge” belonging to the homotopy group $\pi_{N-1}(S_{N-1}) = \mathbb{Z}$. The winding number is calculated by an integral over a $N-1$ -dimensional hypersurface enclosing a N -dimensional volume [17]:

$$\hat{N} = \frac{1}{(N-1)!} \int dS \frac{\epsilon^{abc\dots} \hat{n}^a \otimes \hat{n}^b \otimes \hat{n}^c \otimes \dots}{(N-1)! S_{N-1}} \quad (4)$$

Here ϵ denote the Levi-Civita symbols and $S_{N-1} = 2\pi^{N/2} = (N-2)!!$ the surface of the unit sphere in N dimensions. Since the winding number operator counts the difference between hedgehogs and anti-hedgehogs, its expectation value vanishes, $\langle \hat{N} \rangle = 0$, but its variance $\langle \hat{N}^2 \rangle$ as a function of the enclosed volume yields the desired spectrum of net magnetization fluctuations.

In order to calculate $\langle \hat{N}^2 \rangle$, we make an additional approximation: For a N -dimensional harmonic oscillator $F = \sqrt{2} \hat{F}$, the ground-state probability distribution $p(\mathbf{F}) \propto F^{N-1} \exp(-F^2/2)$ of the amplitude F is peaked around a (for $N > 1$) non-zero value and the relative width of this peak decreases with increasing N . Therefore, we approximate the operator \hat{F} by an exponentially growing classical value $\hat{F} \approx F(t)$ in all expectation values. This semiclassical approximation will become asymptotically exact in the limit $N \rightarrow \infty$, but we expect it to yield qualitatively correct results also in lower dimensions down to $N = 2$, since $p(\mathbf{F})$ is discernibly peaked even for $N = 2$ and the topological defects are mainly determined by the (quantum) fluctuations of \hat{n} (and not of \hat{F}). For example, calculating [analogously to (3)] the contribution of the fastest growing modes to the correlator $\langle \hat{F}^2(\mathbf{r}; t) \hat{F}^2(\mathbf{r}^0; t) \rangle = F^4(t) + 2\langle \hat{F}^2(\mathbf{r}; t) \hat{F}^2(\mathbf{r}^0; t) \rangle$, we see that the accuracy of the semiclassical approximation $\hat{F} \approx F(t)$ increases for large distances $|\mathbf{r} - \mathbf{r}^0|$ and/or large N . Note that all the linearized \hat{F}_a possess independent initial ground states and commute with each other. Therefore, the \hat{n}_a do also commute with each other [so that operator ordering in (4) is not an issue] and with \hat{F} , which ultimately makes possible the semiclassical approximation of $\hat{F} \approx F$.

The above approach enables us to calculate $\langle \hat{N}^2 \rangle$ in arbitrary dimensions $N \geq 2$. After inserting (4) and using

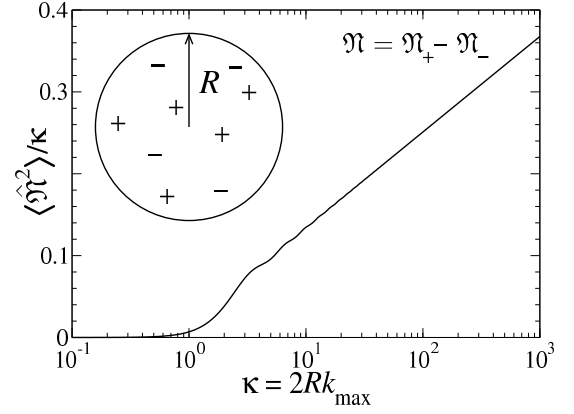


FIG. 2: Scaling of the variance of the winding number $\langle \hat{N}^2 \rangle$ with the sample size R . A logarithmic plot of $\langle \hat{N}^2 \rangle / \kappa$ is used in order to visualize the asymptotic \ln scaling.

the semiclassical approximation $\hat{F}(\mathbf{r}; t) \approx F(t)\hat{n}(\mathbf{r})$, the expectation value can be decomposed into a product of N two-point correlators (3). Let us exemplify this procedure for two spatial dimensions: The transverse magnetization can be decomposed via $\hat{F}_\perp = \hat{F}_x + i\hat{F}_y = \hat{F}e^{i\hat{\phi}}$ into its modulus \hat{F} and phase $\hat{\phi}$ which commute and are both self-adjoint [20]. The winding number (4) reads [21]

$$\hat{N} = \frac{1}{2} \oint_C d\mathbf{l} \cdot \hat{\mathbf{r}} = \frac{1}{2} \oint_C d\mathbf{l} \cdot \frac{\hat{F}_x \hat{F}_y - \hat{F}_y \hat{F}_x}{2\hat{F}^2} \quad (5)$$

Using Eq. (3), replacing $\hat{F} \approx F$, and choosing the contour C as a circle with radius R , we get [22]

$$\langle \hat{N}^2(R) \rangle = \frac{1}{2} \int_0^{2\pi} d\phi \int_0^{2\pi} d\phi' \frac{1}{R^2} \langle \hat{\phi}(\phi) \hat{\phi}(\phi') \rangle \quad (6)$$

with $\kappa = 2Rk_{\text{max}}$, cf. Fig. 2. As anticipated, the characteristic length scale (e.g., typical distance between vortices) is set by the dominant wavelength λ_{max} (instead of the spin healing length λ_s , for example).

The analytical expression (6) enables us to study the large-scale spectrum of the winding number, i.e., the difference between the number of vortices and anti-vortices $\mathcal{N} = \mathcal{N}_+ - \mathcal{N}_-$. Two models for the scaling behavior of \mathcal{N} are commonly discussed in the literature [2, 15]. Assuming a random distribution of vortices and anti-vortices (*random vortex gas* model), the typical difference \mathcal{N} scales with \sqrt{N} . Because the total number $\mathcal{N}_+ + \mathcal{N}_-$ increases proportional to the area R^2 , this model predicts a scaling of $\langle \hat{N}^2 \rangle \propto R^2$ ($N = 2$). Alternatively, the *random phase walk* model assumes a random walk of the phase along the circumference. The accumulated winding number \mathcal{N} scales with \sqrt{R} in this situation, implying a scaling of $\langle \hat{N}^2 \rangle \propto R$. Of course, both models cannot be the final truth (consider the deformation of the circle to a slim ellipse, for example), and it is not

obvious how to generalize the random phase walk model to higher dimensions – but one can compare the different predictions with our approach. For large τ , the expansion $J_1(x) \sim 1 - x^2/2 + \dots$ yields (cf. Fig. 2)

$$\hat{N}^2 \sim \ln \tau; \quad (7)$$

which is close to the scaling predicted by the random phase walk model – but still not quite in agreement due to the additional factor of $\ln \tau$. This extra factor only occurs for $N = 2$ and arises from the slow decay of the two-point correlator (3) at large distances $\langle \psi^\dagger(\mathbf{r}) \psi(\mathbf{r}') \rangle \sim 1/r^{1/2}$, which deviates from a local random phase walk [23]. Although the sample size in [7] is probably not sufficient for extracting the factor $\ln \tau$, this prediction could be tested in future experiments.

Let us study intermediate τ values and compare our results with the experiment [7] by placing a circle with a radius of $R = 5 \mu\text{m}$ into the center of the condensate cloud. Since R is significantly bigger than the spin healing length $\xi_s = 2.4 \mu\text{m}$ but still sufficiently below the planar Thomas-Fermi radii of the cloud ($12.8 \mu\text{m}$ and $167 \mu\text{m}$), the assumptions entering our derivation (such as homogeneity) should provide a reasonably good approximation. For $R = 5 \mu\text{m}$ corresponding to $\tau = 4$, we obtain $\hat{N}^2 \sim \ln \tau = 1.3$, i.e., the probability of finding an (anti-)vortex inside the circle is around $1/3$. In view of the cigar shape of the cloud, we may place several circles in the central region of the condensate such that their mutual distance exceeds the correlation length (typical domain size) of $\xi_m = 2.8 \mu\text{m}$. Since these circles can be considered nearly independent, we would expect at least one vortex in the cloud – in reasonable agreement with [7]. In contrast, the defect density is calculated in Ref. [19] to be $k_{\text{max}}^2 = (4 \mu\text{m})^{-2}$, treating the magnetization as a Gaussian stochastic field. Therefore, a circle with a radius of $R = 2/k_{\text{max}} = 5 \mu\text{m}$ should typically contain one defect. Although the discrepancy ($1/3$ vs. one) is not huge, it already suggests that our results are not quite compatible with Ref. [19], and thus experiment should judge which approach yields the better description. Alternatively, numerical simulations (supplemented by suitable assumptions about the initial noise spectrum) provide a complementary approach [24].

In conclusion, for the example of a spinor Bose gas, we studied the creation of topological defects during the quench from the paramagnetic to the $SO(N)$ -symmetry breaking ferromagnetic phase. For an arbitrary number N of spatial dimensions, we derived a universal expression for the winding number (which only depends on N and the enclosed volume in units of ξ_m^N) and found a logarithmic correction to the scaling law of the random phase walk model for $N = 2$.

R. S. and M. U. acknowledge support by the Emmy Noether Programme of the German Research Foundation (DFG) under grant No. SCHU 1557/1-2. We thank

D. M. Stamper-Kurn and G. E. Volovik for valuable discussions, and acknowledge support by ESF-COSLAB.

schuetz@theory.phy.tu-dresden.de yuwe.fischer@uni-tuebingen.de

-
- [1] T. W. B. Kibble, *J. Phys. A* **9**, 1387 (1976); W. H. Zurek, *Nature* **317**, 505 (1985).
 - [2] M. Hindmarsh and T. W. B. Kibble, *Rep. Prog. Phys.* **58**, 477 (1995); W. H. Zurek, *Phys. Rep.* **276**, 177 (1996).
 - [3] W. H. Zurek, U. Dorner, and P. Zoller, *Phys. Rev. Lett.* **95**, 105701 (2005).
 - [4] J. Stenger *et al.*, *Nature* **396**, 345 (1998).
 - [5] M.-S. Chang *et al.*, *Nature Phys.* **1**, 111 (2005).
 - [6] W. Zhang *et al.*, *Phys. Rev. Lett.* **95**, 180403 (2005).
 - [7] L. E. Sadler, J. M. Higbie, S. R. Leslie, M. Vengalattore, and D. M. Stamper-Kurn, *Nature* **443**, 312 (2006).
 - [8] For brevity, we shall use the terms para- and ferromagnetic synonymously for the more precise descriptions polar paramagnetic and planar ferromagnetic, respectively.
 - [9] J. M. Higbie *et al.*, *Phys. Rev. Lett.* **95**, 050401 (2005).
 - [10] H. Saito and M. Ueda, *Phys. Rev. A* **72**, 023610 (2005).
 - [11] H. Saito, Y. Kawaguchi, and M. Ueda, *Phys. Rev. Lett.* **96**, 065302 (2006).
 - [12] T. Ohmi and K. Machida, *J. Phys. Soc. Jpn.* **67**, 1822 (1998); T.-L. Ho, *Phys. Rev. Lett.* **81**, 742 (1998).
 - [13] Here $\hat{N} = \hat{A}^\dagger \hat{A}$ counts the total number of particles, cf. C. W. Gardiner, *Phys. Rev. A* **56**, 1414 (1997); Y. Castin and R. Dum, *Phys. Rev. A* **57**, 3008 (1998).
 - [14] R. Schützhold, M. Uhlmann, Y. Xu, and U. R. Fischer, *Phys. Rev. Lett.* **97**, 200601 (2006).
 - [15] G. E. Volovik and V. P. Mineev, *Zh. Éksp. Teor. Fiz.* **73**, 767 (1977) [*Sov. Phys. JETP* **46**, 401 (1977) contains a misprint in Eq. (2.4); in the denominator “6”, i.e., (4), was replaced by “8”]; G. E. Volovik, *The Universe in a Helium Droplet* (Oxford University Press, 2003).
 - [16] N. D. Mermin, *Rev. Mod. Phys.* **51**, 591-648 (1979); L. Michel, *Rev. Mod. Phys.* **52**, 617-651 (1979).
 - [17] A. G. Abanov and P. B. Wiegmann, *Nucl. Phys. B* **570**, 685 (2000).
 - [18] C. M. Savage and J. Ruostekoski, *Phys. Rev. A* **68**, 043604 (2003).
 - [19] A. Lamacraft, *Phys. Rev. Lett.* **98**, 160404 (2007).
 - [20] Note that this is distinct from the nonvanishing commutator of density and phase operators resulting from the analogous decomposition of the single-component field operator $\hat{\psi} = \exp[i\hat{\phi}] \hat{\Phi}$, which underlies the definition of conventional momentum/velocity vortices in a fluid.
 - [21] In contrast to spin vortices, domain walls (lines with vanishing F) are not topologically stable for the order parameter considered here. Thus, the domain boundaries observed in [7] are line-like regions with small but not vanishing F , and do not enter Eqs. (4) and (5).
 - [22] The limit of very small τ requires further consideration, which will be presented elsewhere.
 - [23] Observe that the extra factor of $\ln \tau$ in Eq. (7) is only valid within the saddle-point approximation (3), for large times τ (but still in the linear regime [25]). Conversely, keeping the (large) time τ fixed, and considering the limit of ultra-large distances R , the scaling levels off to $\hat{N}^2 \sim \ln R$.
 - [24] H. Saito, Y. Kawaguchi, and M. Ueda, *Phys. Rev. A* **75**, 013621 (2007); preprint arXiv:0704.1377 [cond-

mat.other].

- [25] Note that our results do only describe the initial stage and are, strictly speaking, only valid in the linear regime, i.e., as long as the directions $\mathbf{n}(\mathbf{r})$ are frozen. The sub-

sequent non-linear dynamics, including annihilations of vortex–anti-vortex pairs etc., is not taken into account.